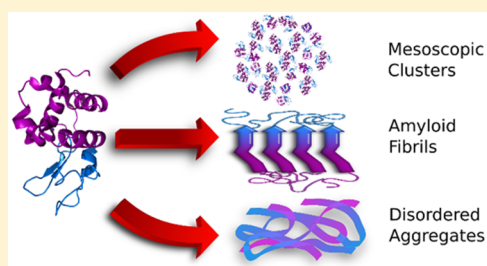


Polymorphism of Lysozyme Condensates

Mohammad S. Safari,[†] Michael C. Byington,[†] Jacinta C. Conrad,^{*,†,‡} and Peter G. Vekilov^{*,†,‡,§}[†]Department of Chemical and Biomolecular Engineering, University of Houston, 4726 Calhoun Road, Houston, Texas 77204-4004, United States[‡]Department of Chemistry, University of Houston, 3585 Cullen Blvd., Houston, Texas 77204-5003, United States

Supporting Information

ABSTRACT: Protein condensates play essential roles in physiological processes and pathological conditions. Recently discovered mesoscopic protein-rich clusters may act as crucial precursors for the nucleation of ordered protein solids, such as crystals, sickle hemoglobin polymers, and amyloid fibrils. These clusters challenge settled paradigms of protein condensation as the constituent protein molecules present features characteristic of both partially misfolded and native proteins. Here we employ the antimicrobial enzyme lysozyme and examine the similarities between mesoscopic clusters, amyloid structures, and disordered aggregates consisting of chemically modified protein. We show that the mesoscopic clusters are distinct from the other two classes of aggregates. Whereas cluster formation and amyloid oligomerization are both reversible, aggregation triggered by reduction of the intramolecular S–S bonds is permanent. In contrast to the amyloid structures, protein molecules in the clusters retain their enzymatic activity. Furthermore, an essential feature of the mesoscopic clusters is their constant radius of less than 50 nm. The amyloid and disordered aggregates are significantly larger and rapidly grow. These findings demonstrate that the clusters are a product of limited protein structural flexibility. In view of the role of the clusters in the nucleation of ordered protein solids, our results suggest that fine-tuning the degree of protein conformational stability is a powerful tool to control and direct the pathways of protein condensation.



INTRODUCTION

Proteins form a variety of condensates in their native environments: crystals, fibrils, dense liquids, and others. In some of these condensates, such as crystals,¹ sickle cell hemoglobin polymers,² and dense liquids,^{3,4} the protein molecules retain their native conformation. In amyloid fibrils, the proteins partially unfold,⁵ whereas amorphous aggregates consist of fully disordered chains with, in some cases, broken intramolecular disulfide bridges.^{6,7} Protein condensates play essential roles in the physiology of living organisms and in the progression of numerous diseases. Insulin crystals, for instance, form in mammalian pancreases to protect the insulin from further proteolysis while it is stored until regulated secretion into the blood serum^{1,8} and, possibly, to increase the degree of conversion from soluble proinsulin.^{1,9} Sickle cell hemoglobin polymers stretch and rigidify the erythrocytes, which, in combination with other factors,¹⁰ lead to obstruction of blood flow and pain crises.^{2,11} Eye lens crystallins form crystals and a dense liquid, which are implicated in age-onset nuclear cataracts.^{12,13} The aggregation of misfolded proteins into oligomers or fibrils is identified as a key process associated with Alzheimer's disease and several other neurological conditions.^{14,15}

Recently, a novel class of protein condensates, mesoscopic protein-rich clusters, was discovered. These clusters exist in solutions of numerous proteins at various pHs, ionicities, temperatures, and compositions.^{16–21} Their diameters are of order 100 nm.^{19–21} Each cluster contains 10^4 – 10^5 protein

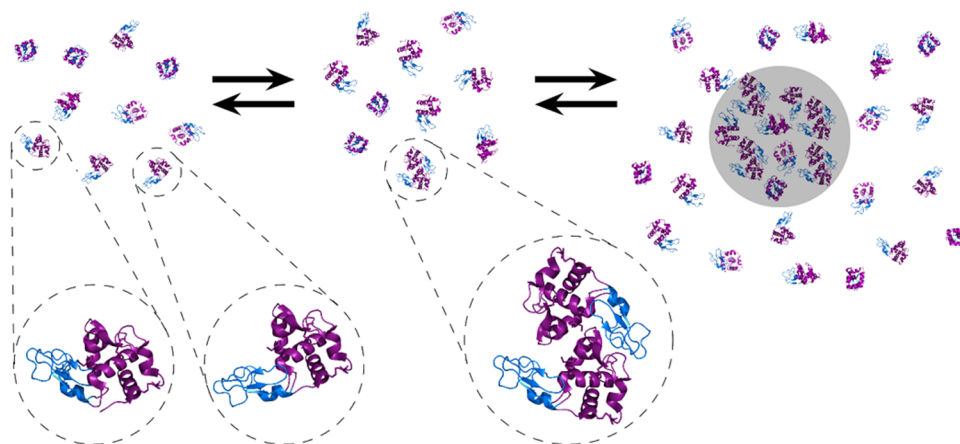
molecules.^{17,19,21,22} The mesoscopic clusters hold 10^{-5} – 10^{-3} of the total soluble protein^{18,23} and the fraction of the solution volume occupied by the cluster population is in the range 10^{-7} – 10^{-3} .^{17–19,21,22} With this small volume, they likely do not affect the macroscopic solution properties.

The mesoscopic clusters have been a focus of recent investigations mostly because they present essential sites for the nucleation of ordered solids of both folded proteins, such as crystals^{21,24–27} and sickle-cell hemoglobin polymers,²⁸ and partially misfolded chains that form amyloid fibrils.^{29–31} Nucleation of ordered protein solids is the crucial first step in the formation of each condensate, and its rate largely determines the rate of condensation. The number of nuclei is limited by a free energy barrier, whereas the growth of the nucleated domains obeys the general chemical kinetics laws.^{2,32–38} A protein solution supersaturated with respect to a condensate overcomes the nucleation barrier by means of localized fluctuations that bring the solute concentration close to that of the incipient phase.³⁹ According to classical nucleation theory, the rarity of successful transitions over the barrier strongly delays nucleation and constrains the overall growth rate of the condensate.⁴⁰ Surprisingly, recent experimental measurements of nucleation rates revealed that they are even lower, by many orders of magnitude, than those predicted

Received: June 2, 2017

Revised: September 6, 2017

Published: September 7, 2017

Scheme 1. Mechanism of Formation of the Mesoscopic Protein-Rich Clusters in Lysozyme Solution^a

^aProtein native monomers, partially unfolded monomers, and domain-swapped dimers are shown in the callouts. The α and β domains, identified as in McCammon, et al.,⁶⁰ are highlighted in purple and blue, respectively. A cluster, highlighted in gray in the right panel, is a region of high protein concentration, into which monomers diffuse and convert to dimers. The dimers migrate back into the solution, where they decay into monomers.¹⁷

by theory.^{41–43} The issue of low nucleation rates and several other unexplained features of protein nucleation kinetics was resolved by the discovery that the mesoscopic protein-rich clusters are a crucial precursor for the nuclei of ordered protein solids.^{21,24–31} This finding underscores the urgent need for in-depth understanding of the structure and formation mechanisms of the mesoscopic clusters.

The mesoscopic clusters challenge basic paradigms of protein condensation. Although the clusters are likely liquid,^{24,25,44} they exist under conditions that are distinct from those of the macroscopic protein dense liquid.^{16,17,22} The clusters are much larger than the prediction of colloid clustering models⁴⁵ that are often applied to protein condensation.^{46–53} The cluster size is steady and independent of the parameters that define the solution thermodynamics, such as pH, ionic strength, and protein concentration.^{18,19,54,55} By contrast, the fraction of the protein captured in the clusters is determined by the protein chemical potential.^{17,18,54,56} A recent theory, supported by experimental evidence, explained several puzzling cluster behaviors.^{17,56–59} This model posits that the mesoscopic clusters consist of a concentrated mixture of intact protein monomers and an additional protein species, emerging at the elevated protein concentration within the clusters.^{17,57,58} Recent experiments indicate that in solutions of the protein lysozyme the clusters are enriched in dimers of partially unfolded protein chains, Scheme 1.^{54,56,59}

This cluster scenario raises several fundamental questions on the cluster composition and mechanisms. Are the mesoscopic clusters similar to amyloid fibrils, which also consist of partially unfolded protein? How different are they from fully disordered proteins, which make up amorphous aggregates? Is the chemical integrity of the protein molecules in the clusters preserved, including the disulfide bonds? In view of the irreversibility of some protein aggregates,⁶¹ is cluster formation reversible? Here, we address these questions by experiments with the protein lysozyme, an antimicrobial enzyme, whose easy availability from hen egg white has allowed the accumulation of a significant database of its biochemical and biophysical properties. Ideally, one would characterize the structure of lysozyme composing the clusters by circular dichroism (CD), Raman, or nuclear magnetic resonance (NMR) spectroscopy, or other direct methods. These

techniques encounter a major challenge when applied to the mesoscopic clusters: the low fraction of the total protein captured in them. Hence, we gauge the degree of lysozyme structural modification in the clusters indirectly. We enforce perturbations of the lysozyme a structure along two axes: a chemical, where we sever the intramolecular disulfide bonds, and structural, where we induce amyloid fibrillation. As a readout, we compare the cluster behaviors to those of disordered aggregates and amyloid fibrils that result, respectively, from structural modifications along these two axes. These comparisons reveal that the mesoscopic clusters are a product of limited structural flexibility of the lysozyme molecules and represent a unique class of condensate, functionally and structurally distinct from those formed after significant structural or chemical perturbation of the protein conformation.

■ EXPERIMENTAL SECTION

Materials and Solutions. Our solutions contained 60 mg mL⁻¹ (unless stated otherwise) hen egg white lysozyme dissolved in 20 mM 4-(2-hydroxyethyl)-1-piperazineethanesulfonic acid (HEPES) buffer at pH 7.8 and no additional components. Details about the sources of protein and other reagents and the solution preparation are provided in SI.

Induction and Characterization of Aggregation. The mesoscopic protein-rich clusters are an intrinsic property of the solution. To assess the role of amyloid structures in cluster formation, we induced lysozyme fibrillation by heat-shocking the protein at 65, 80, or 90 °C for 6 min.^{62–64} The formation of amyloid structures was verified by selective binding of thioflavin T (ThT) and 8-anilino-1-naphthalene-1-sulfonic acid (ANS), detected by fluorescence excited by 442 nm for ThT and 350 nm for ANS. To compare the cluster behaviors with those of aggregates forming after chemical modification of the protein, we reduced the intramolecular disulfide bridges using (tris(2-carboxyethyl)phosphine) (TCEP).^{67,65,67,65} Owing to the low-concentration buffer used, the addition of this acidic reagent lowered the pH by up to 0.2 to 7.6. We removed unreacted TCEP and the products of its oxidation by buffer exchange. To quantify the number of sulfhydryl, SH, groups in the native protein and those formed as a result of S–S bond reduction we used the reaction of SH with Elman's reagent, 5,5'-dithio-bis(2-

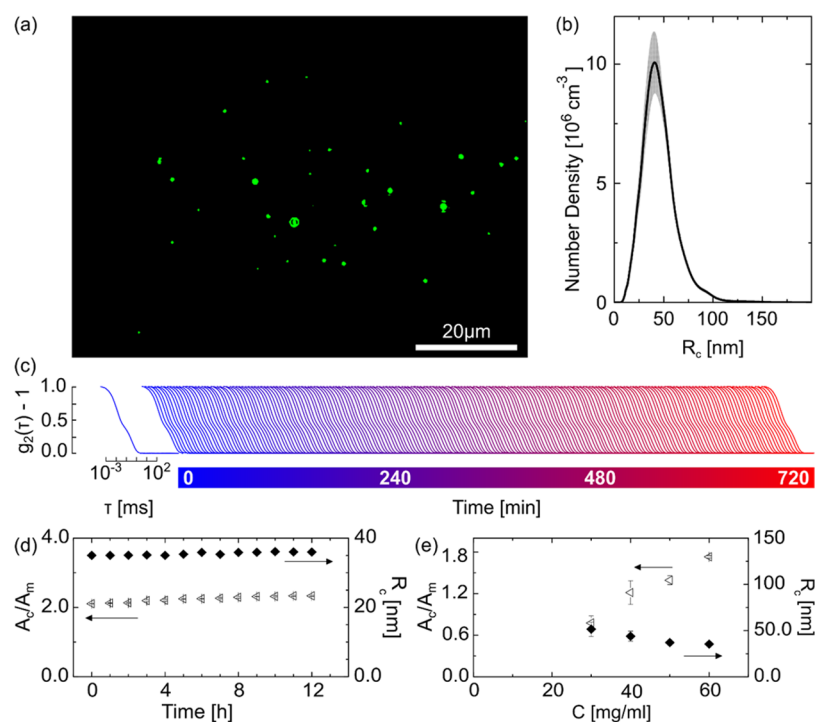


Figure 1. Characterization of the mesoscopic protein-rich clusters by oblique illumination microscopy (OIM) and dynamic light scattering (DLS). (a) A representative OIM image. The observed volume is ca. $120 \times 80 \times 5 \mu\text{m}^3$. Clusters appear as green spots. (b) Number density distribution of the cluster sizes determined by OIM. The average of five determinations in distinct solution volumes is shown. The error bars represent the standard deviation. (c) Intensity correlation functions g_2 of the light scattered by a cluster-containing solution. The two shoulders of g_2 correspond to lysozyme monomers and clusters, respectively.^{54,59,68} g_2 is unchanged over 12 h, indicating that the cluster population is steady. (d) The evolutions of the ratio of the correlation function amplitudes A_c/A_m , which characterizes the fraction of the protein held in the clusters, and the cluster radius R_c , evaluated from g_2 in (c). (e) The dependences of A_c/A_m and R_c on the protein concentration. The values of A_c/A_m and R_c in (d) and (e) represent averages of ten correlation functions; the error bars represent the standard deviation. In (a)–(d), lysozyme concentration was 60 mg mL^{-1} .

nitrobenzoic acid) (DTNB),^{66,67} which yields 5-thio-2-nitrobenzoic acid (TNB) at a concentration equivalent to that of the sulfhydryl. To ensure completeness of the reaction, we waited 20 min after the addition of DTNB.⁶⁷ We quantified the TNB concentration from its absorbance at 412 nm, Figure S1. In addition, we tested the presence of amyloid oligomers in the solution by immunoblotting with ab183461, an antibody that recognizes amyloid structures. The enzymatic activity of lysozyme was evaluated by monitoring the rate of absorbance decrease of a suspension of *Micrococcus lysodeikticus* in the presence of the protein. Further details of these methods are provided in SI.

Characterization of the Aggregates and Clusters. We employed oblique illumination microscopy (OIM) and dynamic light scattering (DLS).^{22,68} Both methods rely on light scattered at wave vectors of order μm^{-1} and probe length scales in the range 10^{-3} – $10 \mu\text{m}$. The Rayleigh law, according to which the scattered intensity scales as the sixth power of the scatterers' sizes, makes these two techniques particularly well suited to study the mesoscopic clusters, which are 50- to 100-fold larger than the monomers, but are present at very low concentration. In OIM, a green laser (532 nm) illuminates a $500 \mu\text{m}$ solution layer at an oblique angle such that the incident beam avoids the lens of a microscope positioned above the sample.^{44,68} The clusters produce bright spots; since the clusters are smaller than the diffraction limit, the spot size accounts for the deviation of the cluster position from the microscope focal plane, Figure 1a. We recorded the Brownian trajectory of a cluster in the image plane and determined its diffusion coefficient and radius using the Stokes–Einstein law

and independently measured solution viscosity.^{44,68} We repeated each characterization five times from distinct solution volumes within the same sample. We plotted the size distribution of the average number density and the standard deviation, determined from the five measurements, in Figure 1b. Further details of this method are provided in SI.^{44,54,68,44,54,68}

In DLS the average size of the clusters or aggregates and the fraction of protein held in the condensates were evaluated from the intensity–intensity correlation functions $g_2(\tau)$, where τ is the lag time. Ten correlation functions of 45 s were collected. All recorded $g_2(\tau)$ possess two distinct shoulders, indicating the presence of two populations of scatterers, Figure 1c. We fit the correlation function with⁶⁸

$$g_2(\tau) - 1 = [A_m \exp(-\tau/\tau_m) + A_c \exp(-\tau/\tau_c)]^2 + \varepsilon(\tau)$$

where τ_m and τ_c are characteristic diffusion times corresponding to the two shoulders, respectively. We attribute the fast diffusion time τ_m to lysozyme monomers and the slow τ_c to the clusters or aggregates.^{22,56,59,68} A_m and A_c are the respective amplitudes, which are proportional to the intensities scattered by the monomers and condensates, respectively, and ε accounts for mechanical, optical, and electronic noise in the signal.^{22,68}

From τ_m and τ_c we compute the diffusivity of the monomer D_m and the hydrodynamic radii of monomer and condensates, R_m and R_c , respectively, using the Stokes–Einstein relation as discussed in the Supporting Information. The ratio of the amplitudes A_c/A_m is a measure of the fraction of protein held in the condensates.^{69,70} In plots characterizing the cluster

population evolution, the average R_c or A_c/A_m are plotted at the time of the first datum point.

RESULTS AND DISCUSSION

Identification and Reversibility of the Mesoscopic Protein-rich Clusters. Lysozyme solutions at low ionic strength are stable against condensation for extended times. One expects that such solutions are homogeneous at all length scales, including the molecular. Surprisingly, observation by OIM of a 60 mg mL⁻¹ (ca. 4 mM) lysozyme solution in 20 mM HEPES (at pH 7.8, at which the ionic strength is 33 mM)⁵⁴ reveals particles suspended in the solution that randomly migrate driven by Brownian collisions, Figure 1a and Supporting Movie 1. Careful examination of all steps in the solution preparation excluded the possibility that these heterogeneities are dust particles or gas bubbles.⁷¹ Recording the diffusion trajectories of individual particles, we determine the radii R_c of individual particles as discussed in SI. The R_c distribution in Figure 1b is relatively narrow, between ca. 10 and ca. 75 nm, with an average size of ca. 40 nm. The particle number density n_c , Figure 1a,b, is very low and corresponds to particle volume fraction $\phi_c = 4\pi(\sum R_c^3 n_c)/3$ of ca. 10⁻⁶.

Characterization of the same solution by DLS reveals the presence of two shoulders in the intensity–intensity correlation function in Figure 1c, with characteristic diffusion times of $\tau_m \approx 20 \mu\text{s}$ and $\tau_c \approx 1 \text{ ms}$. We determine the diffusivities, D_m and D_c , and radii, R_m and R_c , of the two respective scatterers as discussed in SI. After accounting for the intermolecular repulsion,⁵⁴ we obtain $R_m \approx 1.6 \text{ nm}$, the hydrodynamic radius of the lysozyme monomer, whereas the average $R_c = 37 \text{ nm}$ is similar to that found in the OIM experiment (the somewhat higher radius detected by OIM is due to the lower wavelength used in that method, 532 nm, compared to 632.8 nm in DLS, which makes the OIM method more sensitive to larger particles).⁷² The amplitude A_c of the large scatterers is only 2-fold higher than that of the monomers A_m , Figure 1d. The ratio A_c/A_m is proportional to both the concentration ratio of the two solution species and $(R_c/R_m)^6$.^{69,70} As $R_c/R_m \approx \tau_c/\tau_m \approx 50$, the low A_c/A_m ratio is consistent with the low particle concentration detected by OIM. Continuous DLS monitoring of the solution for 12 h revealed that the particle size and the fraction of protein composing the particles, characterized by R_c and A_c/A_m , respectively, are steady, Figure 1c,d.

Several characteristics of the large particles revealed by Figure 1a,b,c,d are unusual for both disordered protein aggregates or emerging domains of a stable phase, such as crystals or dense liquid. The narrow size distribution is inconsistent with both types of aggregation. The concentration and mesoscopic size of the particles are steady over extended times, in sharp contrast to expectations for newly formed phases in which both the domain sizes and the number of new domains grow in time.⁷³ On the other hand, these characteristics are typical of the mesoscopic protein-rich clusters, found in solutions of lysozyme and several other proteins at varying conditions.^{16–21}

We conclude that the particles detected in Figure 1a,b,c,d are mesoscopic lysozyme-rich clusters. The size and concentration of the clusters in Figure 1b,d are consistent with recent *in situ* transmission electron microscopy images.²⁴

A crucial issue in understanding the cluster mechanism is whether the clusters adjust to the parameters of the solution, or represent irreversibly aggregated protein. To test the cluster reversibility, we monitored the dependence of R_c and A_c/A_m on the protein concentration, varied in two ways. First, we

prepared a solution of 60 mg mL⁻¹ and diluted it with buffer to 50, 40, and 30 mg mL⁻¹. Second, we independently prepared solutions with these four concentrations. These experiments test whether the clusters formed at the initial concentration adjust to the diluted solution, and whether newly formed clusters are similar to those resulting from transformation of preexisting condensates. The two methods of solution preparation yielded clusters with identical R_c and A_c/A_m . Figure 1e reveals that R_c increases by ca. 35% as the concentration is diluted from 60 to 30 mg mL⁻¹, whereas the ratio A_c/A_m decreases 3-fold, indicating a similar decrease of the fraction of protein held in the clusters. Diluting a solution of irreversibly aggregated protein would lower the concentration of protein held in the clusters concurrently with the protein concentration, leading to a constant R_c and A_c/A_m . The R_c and A_c/A_m trends in Figure 1e demonstrate that the clusters are reversible aggregates that adjust to the conditions of the hosting solution.

The decoupled behaviors of R_c and A_c/A_m , observed in Figure 1e, are unusual for typical phase transformations, such as freezing or vaporization, in which the size of the incipient domains increases concurrently with the volume of the new phase. On the other hand, such decoupling has been observed previously with the mesoscopic protein-rich clusters.⁵⁴ It has been attributed to the unique nature of the cluster population, whose volume is determined by the thermodynamic balance between the clusters and the solution, whereas the size of its domains results from the kinetics of formation and decay of protein dimers.^{17,54,59,74}

Perturbations of the Protein Structural Integrity. Modeling of the interaction potential between native lysozyme molecules (complementing an earlier theoretical estimate by McCammon and collaborators)^{75–77} suggested that dimers or other oligomers of native lysozyme cannot support the formation of the observed mesoscopic clusters.⁷⁸ Experiments with moderate concentrations of urea and ethanol^{54,56} and with solution shearing,⁵⁹ which destabilize the native conformation, and NMR analyses of cluster-containing and cluster-free solutions⁵⁶ indicate that partial protein unfolding is an integral part of the cluster mechanism. To differentiate the degree of unfolding required for cluster formation from that leading to amyloid fibrillation, we compared the cluster population to amyloid aggregates. To generate amyloid structures, we heated lysozyme solutions to 65, 80, and 90 °C.^{62–64,79–83} To constrain the amount of aggregated protein, we exposed the protein to an elevated temperature for only 6 min.^{62–64,79}

Another aspect of the correlation between conformational flexibility and cluster formation is whether intramolecular S–S bridges are broken during the unfolding that leads to clusters.^{6,7,62,65} To elucidate this issue, we compare the behaviors of the mesoscopic clusters to aggregates induced by reducing the intramolecular S–S bonds using (tris(2-carboxyethyl)phosphine) (TCEP). To evaluate the effects of varying levels of S–S bond disruption, we employ three concentrations of TCEP: 0.1, 0.2, and 0.4 mM. Unreacted TCEP was removed by buffer exchange prior to any additional characterization. We quantify the fraction of S–S bonds converted to sulfhydryl SH by comparing the reaction of the reduced protein with 5,5'-dithio-bis(2-nitrobenzoic acid) (DTNB) to that of glutathione and L-cysteine, which contain one SH group per molecule. The highest fraction of disrupted S–S bonds, after treatment with 0.4 mM TCEP, is 9.8%, Figure 2a, suggesting that the reduction of more than one S–S bond

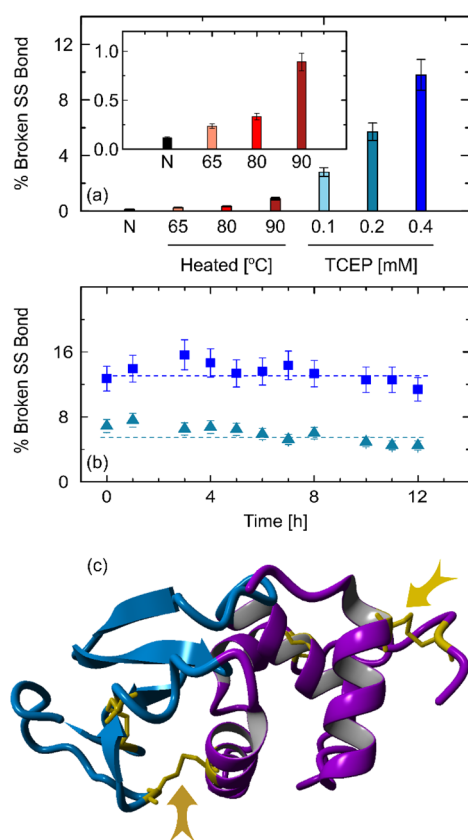


Figure 2. Perturbations of lysozyme structural integrity. (a) Quantification of the sulfhydryl, SH, groups using Elman's reagent, 5,5'-dithio-bis(2-nitrobenzoic acid) (DTNB) in native solutions, N; solutions heated to temperatures shown on the abscissa; and in solutions treated with (tris(2-carboxyethyl)phosphine) (TCEP) at concentrations shown on the abscissa. The average of three independent determinations is plotted; error bars represent the standard deviation. (b) Evolution of the sulfhydryl concentration in lysozyme solutions treated with 0.2 (triangles) and 0.4 (squares) mM TCEP measured after removing the unreacted TCEP by buffer exchange. (c) The structure of lysozyme drawn using by YASARA⁸⁴ and the PDB file 5L9J.⁸⁵ The α and β domains, identified as in McCammon et al.⁶⁰ are highlighted in purple and blue, respectively. S–S bridges are highlighted in gold. Two of the disulfide bridges that appear readily accessible to solvent are indicated with arrows.

per lysozyme molecule is unlikely. The two S–S bonds that appear exposed to the solution, the intra- α -domain C6–C127 and the inter- α - β -domain C76 – C94,⁷ are indicated in Figure 2c.

The steady fraction of broken S–S bonds, Figure 2b, reveals that the resulting SH groups do not rebind into intramolecular S–S bridges or form intermolecular S–S bonds. This observation suggests that the aggregates induced by S–S bond reduction assemble by noncovalent bonds. The enzymatic activity of lysozyme is a sensitive indicator of the structural integrity of the active center of the molecule, located between the α and β domains, illustrated in Figure 2c. Lysozyme hydrolyzes a tetrasaccharide found in Gram-positive bacteria and breaks the glycosidic bond between *n*-acetylmuramic acid and *n*-acetylglucosamine.⁸⁶ We monitored the light absorbance of a bacterial suspension in the presence of native and treated lysozyme, Figure 3a,b. The active enzyme destroys the bacteria, clarifies the suspension, and lowers the absorbance. The activity of TCEP-treated lysozyme is similar, within the error of the

determination, to that of the native protein, Figure 3a. This result is consistent with the low fraction of broken S–S bonds, Figure 2a, and may imply that TCEP reduces the intra- α -domain C6–C127 S-S bond, indicated with the downward arrow in Figure 2c, which has no direct role in the stability of the active center, located between the α and β domains.⁶⁰ Heating to 65 °C for 6 min does not affect the activity of lysozyme, Figure 3b. The activity is significantly lowered after heating to 80 °C. The steady optical density in the presence of lysozyme heated to 90 °C suggests that exposure to this temperature completely destabilizes the active center in the majority of the molecules in the solution. The activity loss due to heating at increased temperature is consistent with previous observations of partial unfolding and fibrillation of lysozyme.⁸⁷

We tested the conformational integrity of heated and TCEP-treated lysozyme using the 1-anilino-8-naphthalenesulfonate (ANS) and thioflavin T (ThT) assays. ANS is a fluorescent probe for the detection of partially unfolded states. ANS binds to hydrophobic sites of proteins, resulting in a blue shift of the fluorescence emission maximum and increase of the fluorescence intensity.^{88,89} ThT binds to β sheet stacks common in amyloid structures and this binding enhances its fluorescence emission;⁹⁰ importantly, ThT is insensitive to lysozyme amyloid oligomers and only interacts with protofibrils and their more complex structures.^{80,81,91} The fluorescent intensities in Figure 3d demonstrate that ANS binding to lysozyme heated to 65 °C is indistinguishable from that of native lysozyme; heating to 80 °C induces binding comparable to that of native lysozyme, indicating that few new hydrophobic sites were exposed to the solution owing to these treatments. ANS strongly binds to lysozyme heated to 90 °C, suggesting numerous exposed hydrophobic sites.

The results on ANS binding in Figure 3c suggest that the degree of exposed hydrophobic patches after treatment with 0.4 mM TCEP is low; it is even lower for protein treated with 0.2 mM TCEP. ANS binding to protein treated with 0.1 mM TCEP is comparable to that of native lysozyme. The results of the ThT assays in Figure 3e,f suggest that the amount of stacked β sheets in the lysozyme treated with TCEP and heated to 65 and 80 °C is similar to that in the native protein, whereas the lysozyme heated to 90 °C presents abundant amyloid structures. Concomitantly, immunoblotting of native, TCEP-treated, and lysozyme heated to 90 °C with an antibody that recognizes amyloid structures, Figure 3g, indicates no amyloid structures in the native protein, weak amyloid response in the TCEP-treated, and pronounced amyloid formation in the heated lysozyme.

Collectively, the results in Figure 3 indicate that disruption of the S–S bonds by TCEP partially unfolds the protein. Limited exposure to 65 °C does not affect the native protein structure, whereas heating to 80 °C leads to partial unfolding that does not progress to amyloid fibrillation. Heating to 90 °C causes the formation of amyloid structures. These responses are in agreement with expectations.^{6,7,62,65,79,87}

Distinct Aggregation Pathways of Structurally Modified Lysozyme. The DLS correlation functions of heated and TCEP-treated solutions possess two shoulders, Figure S2, corresponding to the diffusion of monomers and aggregates, respectively, and similar to those of the native protein in Figure 1c. In solutions treated with 0.1 and 0.2 mM TCEP the monomer diffusivity D_m , determined from the characteristic diffusion time of the fast shoulder τ_m , is similar to the native diffusivity and steady for 12 h, Figure 4a,b. By contrast, in

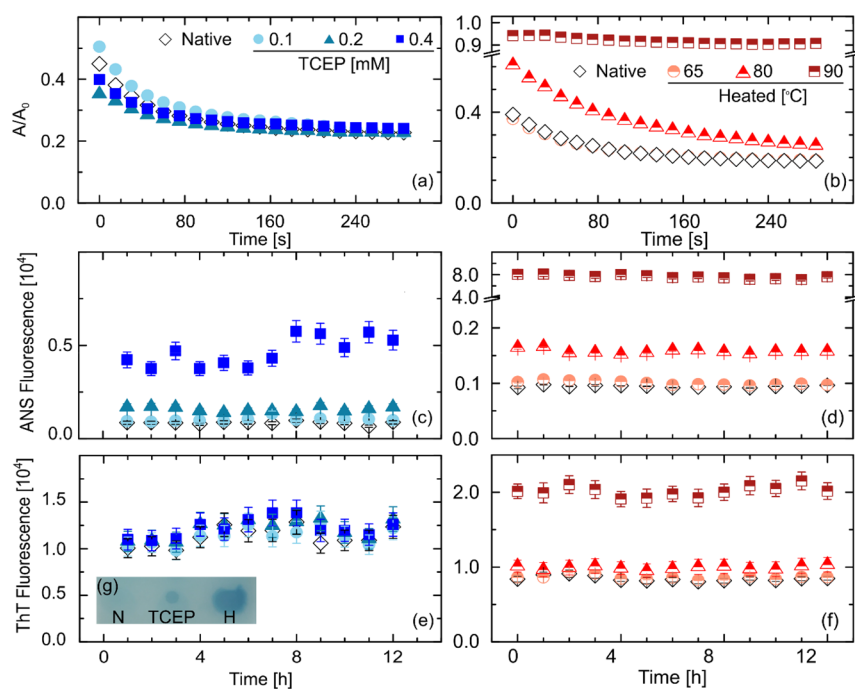


Figure 3. Characterization of the perturbations of the lysozyme molecular structure. (a),(b) Determination of lysozyme enzymatic activity in native and treated solutions. The absorbance A at 450 nm of a suspension of the bacterium *Micrococcus lysodeikticus*, relative to that in a suspension in the absence of lysozyme A_0 , decreases as lysozyme degrades the bacteria. The slopes of the dependences characterize the enzyme activity. (a) In solutions treated with TCEP at concentrations shown in the legend. (b) In solutions heated to temperatures shown in the legend. (c)–(f) Tests of lysozyme conformational integrity after the treatments listed in (a) and (b) using 1-anilino-8-naphthalenesulfonate (ANS), in (c) and (d), and thioflavin T (ThT) in (e) and (f). Fluorescence spectra of lysozyme solutions were recorded in the presence of the respective probe molecule upon excitation with 350 nm, in (c) and (d), and 442 nm, in (e) and (f). Both types of spectra exhibit maxima at about 490 nm. The evolution of the intensity at the maxima is plotted. The time evolutions in (a)–(e) were monitored in four solution samples and the average is plotted. The error bars represent the standard deviation. (g) Dot blot characterization of the binding of an amyloid-recognizing antibody to native (N), treated with 0.4 mM TCEP, and heated to 90 °C (H) lysozyme.

solutions exposed to 0.4 mM TCEP the diffusivity decreases over this time. Lower diffusivity could be an indication of intermolecular attraction.^{54,92,93} Since the fraction of broken S–S bonds in this solution is steady over the tested period, Figure 3a, a slowly emerging attraction is hard to envision. With this, the decreasing D_m trend suggests the assembly of disordered oligomers of up to several molecules that capture a majority of the monomers in the solution.

In solutions heated to 65, 80, and 90 °C, D_m is approximately steady over 12 h, Figure 4b. After heating to 65 and 80 °C, D_m is lower by ca. 5 and 15%, respectively, than that of the native monomer. In combination with the weak ANS signal from hydrophobic interfaces, Figure 3d, and the lack of ThT evidence for amyloid aggregation in Figure 3e, the suppressed D_m suggests enhanced attraction between the lysozyme monomers after partial unfolding that exposes hydrophobic residues to the solvent.⁵⁴ In contrast to these mild effects, exposure to 90 °C lowers D_m ca. 2.5-fold from the value in untreated solutions. The dramatically lower diffusivity of the protein exposed to 90 °C and the strong ThT and ANS responses observed in Figure 3d,f indicate the assembly of the monomers into amyloid oligomers of ca. ten molecules.

The radius R_c of the clusters and aggregates existing in native and treated solutions, Figure 4c,d, is determined from the slow diffusion time τ_c of the DLS correlation function. In solutions treated with 0.1 and 0.2 mM TCEP, the aggregates, which form immediately after solution preparation, are similar in size to the mesoscopic clusters of native lysozyme, Figure 4c. The aggregates formed in 0.4 mM TCEP solution are larger and

capture ca. 2× higher fraction of the total protein, Figure 4e. Over time, the size of the aggregates in solutions treated with 0.2 and 0.4 mM TCEP increases, Figure 4c, in parallel with the increase of the fraction of aggregated protein, Figure 4e. The coupling of R_c and A_c/A_m and the time evolution of the condensate population in solutions with chemically modified protein are in sharp contrast with the respective behaviors of the mesoscopic clusters of native protein, revealed in Figure 1d,e.

Solutions heated to 65 °C exhibit aggregates with R_c somewhat higher than the clusters present in untreated solutions, Figure 4d. The A_c/A_m ratio, Figure 4f, reveals that the aggregates capture a fraction of the protein similar to that in untreated solutions. These comparisons suggest that the aggregates observed in solutions heated to 65 °C represent mesoscopic clusters whose size is enhanced by the destabilization of a fraction of the monomers. The lack of amyloid structures in solutions heated to 80 °C suggests that the heterogeneities detected in these solutions also represent mesoscopic clusters, whose larger size is due to the stronger protein unfolding. The clusters slowly grow, from 160 to 220 nm over 12 h. The concomitant decrease in the fraction of protein captured in the clusters, represented by A_c/A_m , is weak (A_c/A_m is expected to scale with $(R_c/R_m)^3$),^{69,70} suggesting that this evolution represents Ostwald ripening of the clusters, which occurs faster than in previous observations¹⁸ owing to destabilized protein conformation. The amyloid aggregates, present in solutions heated to 90 °C, are ca. 4× larger than the clusters of native lysozyme. Their size is steady over 12 h. The

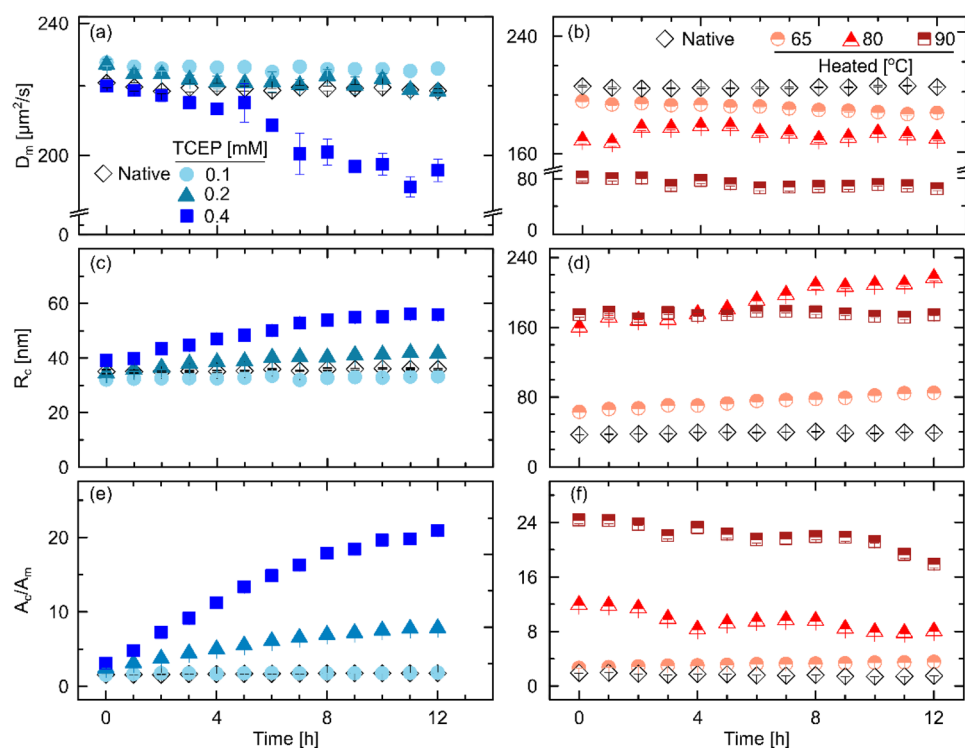


Figure 4. Condensates of native and treated lysozyme. (a),(b) Diffusivity of lysozyme monomers D_m in native solutions and in solutions treated with TCEP at concentrations shown in the legend (a) and after heating for 6 min to temperature shown in the legend in (b). (c),(d) Evolution of the radius R_c of clusters and aggregates detected by DLS after TCEP treatment and heating as in (a) and (b), respectively. (e) and (f) The ratio of the light scattering correlation function amplitudes A_c/A_m for solutions of TCEP-treated, in (e), and heated, in (f) lysozyme. The averages determined from ten correlation functions are plotted; the error bars represent the standard deviation.

steady decrease in the respective A_c/A_m ratio may be due to the formation of complex amyloid structures and their precipitation.⁸⁰ The discussed behaviors indicate persistence of cluster formation, typical of native protein solutions, after short-term exposure to 65 and 80 °C, and amyloid aggregation that requires heating to 90 °C. This conclusion is consistent with the preservation of intact lysozyme α helices upon heating close to the protein melting temperature (extrapolating the pH dependence of the lysozyme melting temperature⁸⁷ to pH 7.8 of our tests suggests that it is between 80 and 90 °C), followed by drastic structure destabilization within additional 10 °C.⁸⁷

The values of R_c and A_c/A_m for native protein in Figure 4c,d are similar to those for solutions treated with 0.1 and 0.2 mM TCEP even though the latter two solutions contain ca. 3 and 6%, respectively, broken intramolecular S–S bonds. The lack of correlation between the broken S–S bonds and the cluster properties suggests that broken S–S bonds, present in 0.2% of the native protein, Figure 2b, are not necessary for cluster formation.⁵⁹ The evolution of R_m and A_c/A_m in lysozyme solutions treated with 0.2 and 0.4 mM TCEP in Figure 4c,d suggests the growth of a population of disordered aggregates of chemically modified lysozyme, or the incorporation of disordered oligomers in the mesoscopic clusters, which increases the cluster size and stabilizes the cluster population. Both scenarios utilize the disordered oligomers, evidenced by the decreasing D_m in Figure 4a, and are compatible with the results of the ANS assays for partial unfolding in Figure 3c.

To assess the applicability of these scenarios, we tested the reversibility of aggregation of structurally modified lysozyme by monitoring the dependence of A_c/A_m on the protein concentration. We prepared a solution of 60 mg mL⁻¹ and

diluted with buffer down to 20 mg mL⁻¹. We mimicked irreversibly aggregated lysozyme by suspending latex particles with radius 100 nm in a lysozyme solution. Diluting this suspension with buffer lowers the concentration of both particles and protein and keeps the ratio A_c/A_m constant, Figure 5a. The fraction of the protein captured in amyloid

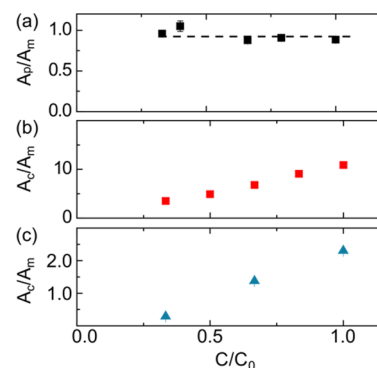


Figure 5. Reversibility of the aggregates formed in heated and TCEP-treated solutions. (a) The ratio A_p/A_m of the amplitudes of the DLS correlation function g_2 from a suspension of latex particles of radius $R_p = 100$ nm in a lysozyme solution with $C_{m,0} = 60$ mg mL⁻¹ as a function of particle concentration. The initial particle concentration $C_{p,0}$ corresponds to volume fraction $\phi_0 = 4 \times 10^{-6}$. A solution with $C_{p,0}$ and $C_{m,0}$ was diluted with 20 mM HEPES buffer so that the ratio C_p/C_m remained constant. (b),(c) The dependence of the ratio A_c/A_m on the protein concentration for solutions heated to 90 °C, in (b), and for solutions treated with 0.2 mM TCEP, in (c). $C_0 = 60$ mg mL⁻¹ in both (b) and (c). The averages determined from ten correlation functions are plotted; the error bars represent the standard deviation.

aggregates decreases significantly upon dilution, Figure 5b, reflecting the reversibility of small amyloid aggregates, seen with several proteins.⁹⁴ The A_c/A_m trend for lysozyme freshly treated with 0.2 mM TCEP indicates that these condensates are reversible, Figure 5c. The observed reversibility implies that the disordered oligomers do not form a separate population of aggregates (aggregation of lysozyme with broken S–S bonds is expected to be irreversible,^{6,7,62,65}) but rather incorporate into the mesoscopic clusters, where they lead to greater cluster size and higher total volume of the cluster population.

Aggregation of Chemically Modified Lysozyme. The evolution of the aggregates in solutions with a higher fraction of broken S–S bonds, induced by treatment with 0.4 mM TCEP in Figure 4c,e, diverges from that in the other tested solutions. For additional evidence for an alternative aggregation mechanism in solutions with high concentration of chemically modified molecules, we explore the cluster size distribution determined by OIM. The data in Figure 6 demonstrate that in

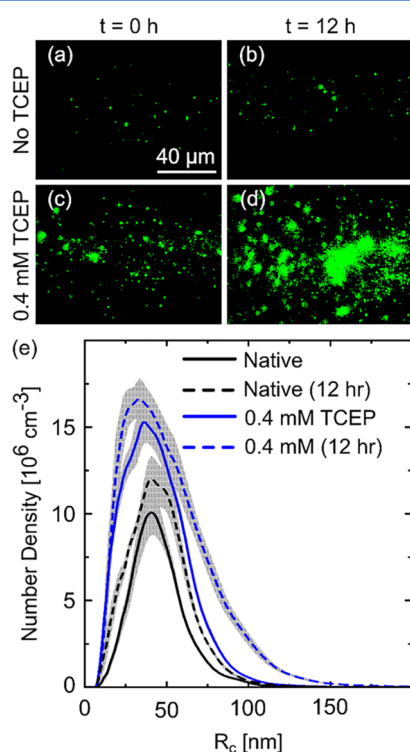


Figure 6. Evolution of aggregates in TCEP-treated solutions. (a)–(d) Representative OIM images from native lysozyme solutions and from solutions treated with 0.4 mM TCEP, shortly after preparation and after 12 h. Clusters appear as green spots. The observed volume is approximately $120 \times 80 \times 5 \mu\text{m}^3$. Lysozyme concentration is 60 mg mL^{-1} in all panels. (e) Number density distributions of the cluster sizes determined by OIM in the four solutions represented in (a)–(d). The average of five determinations in distinct solution volumes is shown; the error bars represent the standard deviation.

solution of native lysozyme, the cluster population 12 h after solution preparation is practically identical to that in freshly prepared solutions. This observation agrees with the data in Figure 1c,d. The average radius of clusters in solutions freshly treated with TCEP is slightly greater than in native solutions, and the cluster concentration is higher by ca. 50%, Figure 6e, consistent with the observations in Figure 4c,d. Importantly, after 12 h, the TCEP-treated solution exhibits a second population of aggregates with radius ca. 90 nm, which exists in

parallel with the mesoscopic clusters present in both native and TCEP-treated solutions, Figure 6d,e. The second population of condensates might be a product of the aggregation of the disordered oligomers, reflected in the decreasing D_m trend in Figure 3a.

We tested the reversibility of aggregation in solutions kept in the presence of 0.4 mM TCEP for 12 h. For this, we prepared a 60 mg mL^{-1} lysozyme solution, applied TCEP, and stored the solution at $22 \text{ }^\circ\text{C}$ for 12 h. We divided this solution into three aliquots that were undiluted and diluted to two final concentrations: 40 and 20 mg mL^{-1} . DLS correlation functions indicate that R_c and A_c/A_m , Figure 7, are larger than in solutions

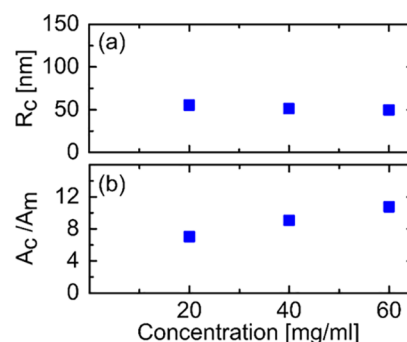


Figure 7. Weak reversibility of aggregates formed in solutions treated with 0.4 mM TCEP and aged for 12 h. (a) The dependence of the aggregate radius R_c in solutions treated with 0.4 mM TCEP on the lysozyme concentration obtained by dilution of the highest concentration sample after incubation for 12 h at $22 \text{ }^\circ\text{C}$. (b) The corresponding dependences of the ratio A_c/A_m . The averages determined from ten correlation functions are plotted; the error bars representing the standard deviation are smaller than the symbol size.

of native protein, Figure 1e, consistent with observations in Figures 4 and 6. R_c is independent and A_c/A_m is a weak function of the dilution ratio, suggesting a weak reversibility of the condensates. The weak reversibility is consistent with the presence of two populations of aggregates, revealed by the OIM size distributions in Figure 6e. Disordered aggregates formed entirely of chemically modified protein are expected to be irreversible;^{6,7,65} however, these aggregates constitute only a fraction of the condensates seen in Figure 6d,e. It appears that the population of mesoscopic clusters, preserved in these solutions after aging in the presence of TCEP, has retained its reversibility.

Collectively, the observations in Figures 4–7 suggest that disordered chains of chemically modified protein form oligomers in the solution that may invade the mesoscopic clusters or assemble into distinct condensates, existing in parallel with the mesoscopic clusters. The disordered oligomers embedded in the clusters modify their properties, but do not affect the cluster reversibility; condensates assembled from oligomers are likely irreversible.

CONCLUSIONS

The results presented here demonstrate that three distinct condensate polymorphs may self-assemble in lysozyme solutions. The selection of condensation pathway is guided by the environmental stress: mesoscopic protein-rich clusters exist at typical laboratory conditions and in solutions heated to 65 or $80 \text{ }^\circ\text{C}$; heating to $90 \text{ }^\circ\text{C}$ for a limited time induces amyloid fibrillation, whereas reduction potential breaks the

intramolecular S–S bonds and leads to disordered aggregates. The mesoscopic protein-rich clusters represent a unique class of condensate: their radius is steady for 12 h at ca. 40 nm, whereas the amyloid structures are as large as 180 nm and the disordered aggregates grow to 60 nm. Another signature behavior of the mesoscopic clusters is that the cluster radius is decoupled from the fraction of protein captured in the clusters.

We show that the partial unfolding of a small fraction of the lysozyme molecules, a necessary precursor for the formation of mesoscopic clusters,^{54,56,59} differs from the unfolding of a large population of molecules leading to amyloid fibrils. This observation supports the notion that the mesoscopic clusters require opening of the hinge between the α and β domains of lysozyme,^{54,56,59} whereas fibrillation is preceded by destabilization of the α helices.^{62,95,96} In accordance with this molecular viewpoint, the enzymatic activity of lysozyme is fully retained in cluster forming solutions, but the protein that assembles into amyloid structures is inactive. Furthermore, we show that breaking of the intramolecular S–S bonds, which are essential for the structural integrity of lysozyme,^{6,7,62,65} is not a prerequisite for cluster formation.

The formation of mesoscopic clusters of lysozyme is reversible and the fraction of protein captured in them adjusts to variation of the concentration of the host solution. The clusters may capture a low concentration of disordered oligomers. High amounts of chemically modified protein, however, assemble into irreversible disordered aggregates that exist in parallel with the mesoscopic clusters.

■ ASSOCIATED CONTENT

Supporting Information

The Supporting Information is available free of charge on the ACS Publications website at DOI: 10.1021/acs.jpcb.7b05425.

Experimental details of the reagents and solutions used; reduction of the protein S–S bridges and quantification of the resulting sulfhydryl groups; characterization of the amyloid and amorphous lysozyme aggregates by DTNB, ThT, and ANS assays; quantification of lysozyme enzymatic activity; and characterization of clusters and aggregates (PDF)

OIM movie of a 60 mg mL⁻¹ (ca. 4 mM) lysozyme solution in 20 mM HEPES (at pH 7.8, at which the ionic strength is 33 mM) with particles suspended in the solution that randomly migrate driven by Brownian collisions (AVI)

■ AUTHOR INFORMATION

Corresponding Authors

*jconrad@uh.edu.

*vekilov@uh.edu.

ORCID

Jacinta C. Conrad: 0000-0001-6084-4772

Peter G. Vekilov: 0000-0002-3424-8720

Notes

The authors declare no competing financial interest.

■ ACKNOWLEDGMENTS

We thank Dominique Maes and Zhiqing Wang for valuable discussions of protein conformational stability. This work was supported by grants from NASA (NNX14AD68G and

NNX14AE79G), NSF (MCB-1518204, DMR-1710354, and DMR-1131155), and the Welch Foundation (E-1869).

■ REFERENCES

- (1) Dodson, G.; Steiner, D. The role of assembly in insulin's biosynthesis. *Curr. Opin. Struct. Biol.* **1998**, *8* (2), 189–194.
- (2) Eaton, W. A.; Hofrichter, J. Sick cell hemoglobin polymerization. In *Advances in protein chemistry*; Anfinsen, C. B., Edsall, J. T., Richards, F. M., Eisenberg, D. S., Eds.; Academic Press: San Diego, 1990; Vol. 40, pp 63–279.
- (3) Brangwynne, C. P. Phase transitions and size scaling of membrane-less organelles. *J. Cell Biol.* **2013**, *203* (6), 875–881.
- (4) Liu, C.; Asherie, N.; Lomakin, A.; Pande, J.; Ogun, O.; Benedek, G. B. Phase separation in aqueous solutions of lens gamma-crystallins: special role of gamma s. *Proc. Natl. Acad. Sci. U. S. A.* **1996**, *93* (1), 377–382.
- (5) Dobson, C. M. Protein folding and misfolding. *Nature* **2003**, *426*, 884–890.
- (6) Yang, M.; Dutta, C.; Tiwari, A. Disulfide-bond scrambling promotes amorphous aggregates in lysozyme and bovine serum albumin. *J. Phys. Chem. B* **2015**, *119* (10), 3969–3981.
- (7) Guez, V.; Roux, P.; Navon, A.; Goldberg, M. E. Role of individual disulfide bonds in hen lysozyme early folding steps. *Protein Sci.* **2002**, *11* (5), 1136–1151.
- (8) Halban, P.; Mutkoski, R.; Dodson, G.; Orci, L. Resistance of the insulin crystal to lysosomal proteases: implications for pancreatic B-cell crinophagy. *Diabetologia* **1987**, *30* (5), 348–353.
- (9) Carroll, R. J.; Hammer, R. E.; Chan, S. J.; Swift, H. H.; Rubenstein, A. H.; Steiner, D. F. A mutant human proinsulin is secreted from islets of Langerhans in increased amounts via an unregulated pathway. *Proc. Natl. Acad. Sci. U. S. A.* **1988**, *85* (23), 8943–8947.
- (10) Hebbel, R. P.; Osarogiagbon, R.; Kaul, D. The endothelial biology of sickle cell disease: inflammation and a chronic vasculopathy. *Microcirculation* **2004**, *11* (2), 129–151.
- (11) Mozzarelli, A.; Hofrichter, J.; Eaton, W. A. Delay time in hemoglobin S polymerization prevents most of the cells from sickling in vivo. *Science* **1987**, *237*, 500–506.
- (12) Asherie, N.; Pande, J.; Pande, A.; Zarutskie, J. A.; Lomakin, J.; Lomakin, A.; Ogun, O.; Stern, L. J.; King, J.; Benedek, G. B. Enhanced crystallization of the Cys18 to Ser mutant of bovine gammaB Crystallin. *J. Mol. Biol.* **2001**, *314* (4), 663–369.
- (13) Benedek, G. B.; Pande, J.; Thurston, G. M.; Clark, J. I. Theoretical and experimental basis for the inhibition of cataract. *Prog. Retinal Eye Res.* **1999**, *18* (3), 391–402.
- (14) Irvine, G. B.; El-Agnaf, O. M.; Shankar, G. M.; Walsh, D. M. Protein aggregation in the brain: the molecular basis for Alzheimer's and Parkinson's diseases. *Mol. Med.* **2008**, *14* (7–8), 451–464.
- (15) Hamley, I. W. The Amyloid Beta Peptide: A chemist's perspective. Role in Alzheimer's and fibrillization. *Chem. Rev.* **2012**, *112* (10), 5147–5192.
- (16) Gliko, O.; Neumaier, N.; Pan, W.; Haase, I.; Fischer, M.; Bacher, A.; Weinkauf, S.; Vekilov, P. G. A metastable prerequisite for the growth of lumazine synthase crystals. *J. Am. Chem. Soc.* **2005**, *127*, 3433–3438.
- (17) Pan, W.; Vekilov, P. G.; Lubchenko, V. The origin of anomalous mesoscopic phases in protein solutions. *J. Phys. Chem. B* **2010**, *114*, 7620–7630.
- (18) Li, Y.; Lubchenko, V.; Vorontsova, M. A.; Filobelo, L.; Vekilov, P. G. Ostwald-like ripening of the anomalous mesoscopic clusters in protein solutions. *J. Phys. Chem. B* **2012**, *116* (35), 10657–10664.
- (19) Gliko, O.; Pan, W.; Katsonis, P.; Neumaier, N.; Galkin, O.; Weinkauf, S.; Vekilov, P. G. Metastable liquid clusters in super- and undersaturated protein solutions. *J. Phys. Chem. B* **2007**, *111* (12), 3106–3114.
- (20) Schubert, R.; Meyer, A.; Baitan, D.; Dierks, K.; Perbandt, M.; Betzel, C. Real-time observation of protein dense liquid cluster evolution during nucleation in protein crystallization. *Cryst. Growth Des.* **2017**, *17* (3), 954–958.

- (21) Sleutel, M.; Van Driessche, A. E. Role of clusters in nonclassical nucleation and growth of protein crystals. *Proc. Natl. Acad. Sci. U. S. A.* **2014**, *111* (5), E546–E553.
- (22) Pan, W.; Galkin, O.; Filobelo, L.; Nagel, R. L.; Vekilov, P. G. Metastable mesoscopic clusters in solutions of sickle cell hemoglobin. *Biophys. J.* **2007**, *92* (1), 267–277.
- (23) Uzunova, V.; Pan, W.; Lubchenko, V.; Vekilov, P. G. Control of the nucleation of sickle cell hemoglobin polymers by free hematin. *Faraday Discuss.* **2012**, *159* (1), 87–104.
- (24) Yamazaki, T.; Kimura, Y.; Vekilov, P. G.; Furukawa, E.; Shirai, M.; Matsumoto, H.; Van Driessche, A. E. S.; Tsukamoto, K. Two types of amorphous protein particles facilitate crystal nucleation. *Proc. Natl. Acad. Sci. U. S. A.* **2017**, *114*, 2154–2159.
- (25) Maes, D.; Vorontsova, M. A.; Potenza, M. A. C.; Sanvito, T.; Sleutel, M.; Giglio, M.; Vekilov, P. G. Do protein crystals nucleate within dense liquid clusters? *Acta Crystallogr., Sect. F: Struct. Biol. Commun.* **2015**, *71* (7), 815–822.
- (26) ten Wolde, P. R.; Frenkel, D. Enhancement of protein crystal nucleation by critical density fluctuations. *Science* **1997**, *277*, 1975–1978.
- (27) Giegé, R. A historical perspective on protein crystallization from 1840 to the present day. *FEBS J.* **2013**, *280* (24), 6456–6497.
- (28) Galkin, O.; Pan, W.; Filobelo, L.; Hirsch, R. E.; Nagel, R. L.; Vekilov, P. G. Two-step mechanism of homogeneous nucleation of sickle cell hemoglobin polymers. *Biophys. J.* **2007**, *93*, 902–913.
- (29) Krishnan, R.; Lindquist, S. L. Structural insights into a yeast prion illuminate nucleation and strain diversity. *Nature* **2005**, *435* (7043), 765–772.
- (30) Luiken, J. A.; Bolhuis, P. G. Prediction of a stable associated liquid of short amyloidogenic peptides. *Phys. Chem. Chem. Phys.* **2015**, *17* (16), 10556–10567.
- (31) Ruff, K.; Khan, S.; Pappu, R. A coarse-grained model for polyglutamine aggregation modulated by amphipathic flanking sequences. *Biophys. J.* **2014**, *107* (5), 1226–1235.
- (32) Lomakin, A.; Chung, D. S.; Benedek, G. B.; Kirschner, D. A.; Teplow, D. B. On the nucleation and growth of amyloid β -protein fibrils: detection of nuclei and quantification of rate constants. *Proc. Natl. Acad. Sci. U. S. A.* **1996**, *93*, 1125–1129.
- (33) Auer, S.; Ricchiuto, P.; Kashchiev, D. Two-step nucleation of amyloid fibrils: omnipresent or not? *J. Mol. Biol.* **2012**, *422* (5), 723–730.
- (34) Saric, A.; Chebaro, Y. C.; Knowles, T. P. J.; Frenkel, D. Crucial role of nonspecific interactions in amyloid nucleation. *Proc. Natl. Acad. Sci. U. S. A.* **2014**, *111* (50), 17869–17874.
- (35) Vekilov, P. G. Phase transitions of folded proteins. *Soft Matter* **2010**, *6*, 5254–5272.
- (36) Ferrone, F. A.; Hofrichter, H.; Eaton, W. A. Kinetics of sickle cell hemoglobin polymerization I. Studies using temperature jump and laser photolysis techniques. *J. Mol. Biol.* **1985**, *183*, 591–610.
- (37) Broide, M. L.; Berland, C. R.; Pande, J.; Ogun, O. O.; Benedek, G. B. Binary liquid phase separation of lens proteins solutions. *Proc. Natl. Acad. Sci. U. S. A.* **1991**, *88*, 5660–5664.
- (38) Shah, M.; Galkin, O.; Vekilov, P. G. Smooth transition from metastability to instability in phase separating protein solutions. *J. Chem. Phys.* **2004**, *121*, 7505–7512.
- (39) Kashchiev, D. *Nucleation. Basic theory with applications*; Butterworth, Heinemann: Oxford, 2000; p 529.
- (40) Gibbs, J. W. On the equilibrium of heterogeneous substances, First Part. *Trans. Connect. Acad. Sci.* **1876**, *3*, 108–248.
- (41) Dorsaz, N.; Filion, L.; Smallenburg, F.; Frenkel, D. Spiers Memorial Lecture: Effect of interaction specificity on the phase behaviour of patchy particles. *Faraday Discuss.* **2012**, *159* (1), 9–21.
- (42) Auer, S.; Frenkel, D. Numerical prediction of absolute crystallization rates in hard-sphere colloids. *J. Chem. Phys.* **2004**, *120* (6), 3015–3029.
- (43) Vekilov, P. G. Nucleation. *Cryst. Growth Des.* **2010**, *10* (12), 5007–5019.
- (44) Vorontsova, M. A.; Vekilov, P. G.; Maes, D. Characterization of the diffusive dynamics of particles with time-dependent asymmetric microscopy intensity profiles. *Soft Matter* **2016**, *12* (33), 6926–6936.
- (45) Hutchens, S. B.; Wang, Z.-G. Metastable cluster intermediates in the condensation of charged macromolecule solutions. *J. Chem. Phys.* **2007**, *127*, 084912.
- (46) Stradner, A.; Sedgwick, H.; Cardinaux, F.; Poon, W. C. K.; Egelhaaf, S. U.; Schurtenberger, P. Equilibrium cluster formation in concentrated protein solutions and colloids. *Nature* **2004**, *432* (7016), 492–495.
- (47) Porcar, L.; Falus, P.; Chen, W.-R.; Faraone, A.; Fratini, E.; Hong, K.; Baglioni, P.; Liu, Y. Formation of the dynamic clusters in concentrated lysozyme protein solutions. *J. Phys. Chem. Lett.* **2010**, *1* (1), 126–129.
- (48) Erlkamp, M.; Grobelny, S.; Faraone, A.; Czeslik, C.; Winter, R. Solvent effects on the dynamics of amyloidogenic insulin revealed by neutron spin echo spectroscopy. *J. Phys. Chem. B* **2014**, *118* (12), 3310–3316.
- (49) Johnston, K. P.; Maynard, J. A.; Truskett, T. M.; Borwankar, A. U.; Miller, M. A.; Wilson, B. K.; Dinin, A. K.; Khan, T. A.; Kaczorowski, K. J. Concentrated dispersions of equilibrium protein nanoclusters that reversibly dissociate into active monomers. *ACS Nano* **2012**, *6* (2), 1357–1369.
- (50) Borwankar, A. U.; Dinin, A. K.; Laber, J. R.; Twu, A.; Wilson, B. K.; Maynard, J. A.; Truskett, T. M.; Johnston, K. P. Tunable equilibrium nanocluster dispersions at high protein concentrations. *Soft Matter* **2013**, *9* (6), 1766–1771.
- (51) Soraruf, D.; Roosen-Runge, F.; Grimaldo, M.; Zanini, F.; Schweins, R.; Seydel, T.; Zhang, F.; Roth, R.; Oettel, M.; Schreiber, F. Protein cluster formation in aqueous solution in the presence of multivalent metal ions - a light scattering study. *Soft Matter* **2014**, *10* (6), 894–902.
- (52) Yearley, E. J.; Godfrin, P.; Paul, D.; Perevozchikova, T.; Zhang, H.; Falus, P.; Porcar, L.; Nagao, M.; Curtis, J.; Joseph, E.; Gawande, P.; Taing, R.; et al. Observation of small cluster formation in concentrated monoclonal antibody solutions and its implications to solution viscosity. *Biophys. J.* **2014**, *106* (8), 1763–1770.
- (53) Cardinaux, F.; Stradner, A.; Schurtenberger, P.; Sciortino, F.; Zaccarelli, E. Modeling equilibrium clusters in lysozyme solutions. *EPL (Europhysics Letters)* **2007**, *77* (4), 48004.
- (54) Vorontsova, M. A.; Chan, H. Y.; Lubchenko, V.; Vekilov, P. G. Lack of dependence of the sizes of the mesoscopic protein clusters on electrostatics. *Biophys. J.* **2015**, *109* (9), 1959–1968.
- (55) Uzunova, V. V.; Pan, W.; Galkin, O.; Vekilov, P. G. Free heme and the polymerization of sickle cell hemoglobin. *Biophys. J.* **2010**, *99* (6), 1976–1985.
- (56) Vorontsova, M. A.; Maes, D.; Vekilov, P. G. Recent advances in the understanding of two-step nucleation of protein crystals. *Faraday Discuss.* **2015**, *179* (0), 27–40.
- (57) Lutsko, J. F.; Nicolis, G. Mechanism for the stabilization of protein clusters above the solubility curve. *Soft Matter* **2016**, *12*, 93–98.
- (58) Lutsko, J. F., Mechanism for the stabilization of protein clusters above the solubility curve: the role of non-ideal chemical reactions. *J. Phys.: Condens. Matter* **2016**, *28*, 244020.
- (59) Byington, M. C.; Safari, M. S.; Conrad, J. C.; Vekilov, P. G. Protein conformational flexibility enables the formation of dense liquid clusters: tests using solution shear. *J. Phys. Chem. Lett.* **2016**, *7*, 2339–2345.
- (60) McCammon, J. A.; Gelin, B. R.; Karplus, M.; Wolynes, P. G. The hinge-bending mode of lysozyme. *Nature* **1976**, *262*, 325–326.
- (61) Kendrick, B. S.; Carpenter, J. F.; Cleland, J. L.; Randolph, T. W. A transient expansion of the native state precedes aggregation of recombinant human interferon- γ . *Proc. Natl. Acad. Sci. U. S. A.* **1998**, *95* (24), 14142–14146.
- (62) Canet, D.; Last, A. M.; Tito, P.; Sunde, M.; Spencer, A.; Archer, D. B.; Redfield, C.; Robinson, C. V.; Dobson, C. M. Local cooperativity in the unfolding of an amyloidogenic variant of human lysozyme. *Nat. Struct. Biol.* **2002**, *9* (4), 308–315.

- (63) Frare, E.; Polverino de Laureto, P.; Zurdo, J.; Dobson, C. M.; Fontana, A. A highly amyloidogenic region of hen lysozyme. *J. Mol. Biol.* **2004**, *340* (5), 1153–1165.
- (64) Fändrich, M. Oligomeric intermediates in amyloid formation: structure determination and mechanisms of toxicity. *J. Mol. Biol.* **2012**, *421* (4–5), 427–440.
- (65) Dombkowski, A. A.; Sultana, K. Z.; Craig, D. B. Protein disulfide engineering. *FEBS Lett.* **2014**, *588* (2), 206–212.
- (66) Ellman, G. L. Tissue sulfhydryl groups. *Arch. Biochem. Biophys.* **1959**, *82* (1), 70–77.
- (67) Riener, C. K.; Kada, G.; Gruber, H. J. Quick measurement of protein sulfhydryls with Ellman's reagent and with 4,4'-dithiodipyridine. *Anal. Bioanal. Chem.* **2002**, *373* (4), 266–276.
- (68) Li, Y.; Lubchenko, V.; Vekilov, P. G. The use of dynamic light scattering and Brownian microscopy to characterize protein aggregation. *Rev. Sci. Instrum.* **2011**, *82*, 053106.
- (69) Ford, N. C. Biochemical applications of laser Rayleigh-scattering. *Chemica Scripta* **1972**, *2* (5), 193.
- (70) Chen, F. C.; Tschamruter, W.; Schmidt, D.; Chu, B. Experimental evaluation of macromolecular polydispersity in intensity correlation spectroscopy using the cumulant expansion technique. *J. Chem. Phys.* **1974**, *60* (4), 1675–1676.
- (71) Sedláč, M.; Rak, D. Large-scale inhomogeneities in solutions of low molar mass compounds and mixtures of liquids: supramolecular structures or nanobubbles? *J. Phys. Chem. B* **2013**, *117* (8), 2495–2504.
- (72) Safari, M. S.; Vorontsova, M. A.; Poling-Skutvik, R.; Vekilov, P. G.; Conrad, J. C. Differential dynamic microscopy of weakly scattering and polydisperse protein-rich clusters. *Phys. Rev. E* **2015**, *92* (4), 042712.
- (73) Chaikin, P. M.; Lubensky, T. C. *Principles of condensed matter physics*; Cambridge University Press: Cambridge, 1995.
- (74) Kolomeisky, A. B. Staying together: protein molecules in mesoscopic clusters. *Biophys. J.* **2015**, *109* (9), 1759–1760.
- (75) Elcock, A. H.; McCammon, J. A. Identification of protein oligomerization states by analysis of interface conservation. *Proc. Natl. Acad. Sci. U. S. A.* **2001**, *98* (6), 2990–2994.
- (76) Elcock, A. H.; Sept, D.; McCammon, J. A. Computer Simulation of Protein–Protein Interactions. *J. Phys. Chem. B* **2001**, *105* (8), 1504–1518.
- (77) Elcock, A. H.; McCammon, J. A. Calculation of weak protein-protein interactions: the pH dependence of the second virial coefficient. *Biophys. J.* **2001**, *80* (2), 613–625.
- (78) Chan, Ho Y.; Lankevich, V.; Vekilov, P. G.; Lubchenko, V. Anisotropy of the Coulomb interaction between folded proteins: consequences for mesoscopic aggregation of lysozyme. *Biophys. J.* **2012**, *102* (8), 1934–1943.
- (79) Frare, E.; Mossuto, M. F.; de Laureto, P. P.; Tolin, S.; Menzer, L.; Dumoulin, M.; Dobson, C. M.; Fontana, A. Characterization of oligomeric species on the aggregation pathway of human lysozyme. *J. Mol. Biol.* **2009**, *387* (1), 17–27.
- (80) Hill, S. E.; Robinson, J.; Matthews, G.; Muschol, M. Amyloid protofibrils of lysozyme nucleate and grow via oligomer fusion. *Biophys. J.* **2009**, *96* (9), 3781–3790.
- (81) Hill, S. E.; Richmond, T.; Muschol, M. M. Denatured-state conformation as regulator of amyloid assembly pathways? *Biophys. J.* **2010**, *98* (3), 17a–17a.
- (82) Hill, S. E.; Miti, T.; Richmond, T.; Muschol, M. Spatial extent of charge repulsion regulates assembly pathways for lysozyme amyloid fibrils. *PLoS One* **2011**, *6* (4), e18171.
- (83) Muschol, M.; Hill, S. E.; Ciesla, M.; Robeel, R.; Miti, T.; Foley, J.; Persichilli, C.; Mulaj, M.; Raynes, R.; Westerheide, S. Structural evolution of oligomeric vs. oligomer-free amyloid fibril growth. *Biophys. J.* **2013**, *104* (2), 49a–49a.
- (84) Krieger, E.; Vriend, G. New ways to boost molecular dynamics simulations. *J. Comput. Chem.* **2015**, *36* (13), 996–1007.
- (85) Crosas, E.; Castellvi, A.; Crespo, I.; Fulla, D.; Gil-Ortiz, F.; Fuertes, G.; Kamma-Lorger, C. S.; Malfois, M.; Aranda, M. A. G.; Juanhuix, J. Uridine as a new scavenger for synchrotron-based structural biology techniques. *J. Synchrotron Radiat.* **2017**, *24* (1), 53–62.
- (86) Ibrahim, H. R.; Matsuzaki, T.; Aoki, T. Genetic evidence that antibacterial activity of lysozyme is independent of its catalytic function. *FEBS Lett.* **2001**, *506* (1), 27–32.
- (87) Arnaudov, L. N.; de Vries, R. Thermally induced fibrillar aggregation of hen egg white lysozyme. *Biophys. J.* **2005**, *88* (1), 515–526.
- (88) Gasymov, O. K.; Glasgow, B. J. ANS Fluorescence: potential to augment the identification of the external binding sites of proteins. *Biochim. Biophys. Acta, Proteins Proteomics* **2007**, *1774* (3), 403–411.
- (89) Hawe, A.; Sutter, M.; Jiskoot, W. Extrinsic fluorescent dyes as tools for protein characterization. *Pharm. Res.* **2008**, *25* (7), 1487–1499.
- (90) Biancalana, M.; Koide, S. Molecular mechanism of thioflavin-T binding to amyloid fibrils. *Biochim. Biophys. Acta, Proteins Proteomics* **2010**, *1804* (7), 1405–1412.
- (91) Persichilli, C.; Hill, S. E.; Mast, J.; Muschol, M. Does Thioflavin-T detect oligomers formed during amyloid fibril assembly. *Biophys. J.* **2011**, *100* (3), 538–538.
- (92) Ackerson, B. J. Correlations for interacting Brownian particles 0.2. *J. Chem. Phys.* **1978**, *69* (2), 684–690.
- (93) Muschol, M.; Rosenberger, F. Interaction in undersaturated and supersaturated lysozyme solutions: static and dynamic light scattering results. *J. Chem. Phys.* **1995**, *103*, 10424–10432.
- (94) Cabriolu, R.; Auer, S. Amyloid fibrillation kinetics: insight from atomistic nucleation theory. *J. Mol. Biol.* **2011**, *411* (1), 275–285.
- (95) Buell, A. K.; Dhulesia, A.; Mossuto, M. F.; Cremades, N.; Kumita, J. R.; Dumoulin, M.; Welland, M. E.; Knowles, T. P. J.; Salvatella, X.; Dobson, C. M. Population of nonnative states of lysozyme variants drives amyloid fibril formation. *J. Am. Chem. Soc.* **2011**, *133* (20), 7737–7743.
- (96) Mossuto, M. F.; Dhulesia, A.; Devlin, G.; Frare, E.; Kumita, J. R.; de Laureto, P. P.; Dumoulin, M.; Fontana, A.; Dobson, C. M.; Salvatella, X. The non-core regions of human lysozyme amyloid fibrils influence cytotoxicity. *J. Mol. Biol.* **2010**, *402* (5), 783–796.